5) The spreading boundaries of the high-temperature, partially ionized jet were found to depart from the conical shape of isothermal jets

References

[1] Forstall, W, Jr and Shapiro, A H, "Momentum and mass transfer in coaxial gas jets, J Appl Mech **10**, 399–408 (December 1950)

[2] Pai, S I, *Fluid Dynamics of Jets* (D Van Nostrand Co, Inc, Princeton, N J, 1954), Chaps 5–7, pp 96–173

[3] Willis, D R and Glassman, I, "The mixing of unbounded coaxial compressible streams,' Jet Propulsion **27**, 1241–1248 (1957)

[4] Pitkin, E T and Glassman, I, "Experimental mixing profiles of a Mach 2 6 free jet," J Aerospace Sci **25**, 791–792 (1958)

[5] Grey, J, Jacobs, P F, and Sherman, M P, "Calorimetric probe for the measurement of extremely high temperatures,' Rev Sci Instr **33**, 738–741 (July 1962)

[6] Grey, J, "Thermodynamic methods of high temperature measurement," Am Soc Mech Engrs Annual Meeting, Philadelphia, Pa (November 18, 1963); also Instr Soc Am (submitted for publication)

[7] Sherman, M P, Jacobs, P F, and Grey, J, "Analytical and experimental study of radiation from an argon arcjet," Princeton Univ Aeronaut Eng Rept 658 (July 1963)

[8] Grey, J, Sherman, M P, and Jacobs, P F, "A collimated total radiation probe for arcjet measurements,' Inst Elec Electron Engrs Intern Symp Plasma Phenomena and Measurements, San Diego, Calif (October 31, 1963); also Inst Elec Electron Engrs Trans Nucl Sci (January 1964)

[9] Grey, J and Jacobs, P F, ' Turbulent mixing in a partially ionized gas," Princeton Univ Aeronaut Eng Rept 625 (September 1962)

[10] Sherman, M P and Grey, J, "The degree of approach to equilibrium in an atmospheric-pressure arcjet using argon,' Princeton Univ Aeronaut Eng Rept 645 (April 1963)

[11] Cann, G L and Ducati, A C, "Argon mollier chart,' Air Force Office Sci Res AF 49(638)-54 (February 1959)

[12] Bosnjakovic, R, Springe, W, Knoche, K F, and Burgholte, P, "Mollier Enthalpie—Entropie Diagramm für Argon Plasma im Gleichgewicht,' transl by J F Gross, Wärmetechnische Institut, Technische Hochschule, Braunschweig (August 1958)

[13] Squire, H B and Trouncer, J, "Round jets in a general stream,' Brit Aeronaut Res Comm Repts and Memo 1974, pp 9–31 (January 1944)

[14] Corrsin, S and Uberoi, M S, "Further experiments on the flow and heat transfer in a heated turbulent air jet," NACA Rept 998 (1950)

MARCH 1964 AIAA JOURNAL VOL 2, NO 3

Laminar Heat Transfer to Spherically Blunted Cones at Hypersonic Conditions

B J Griffith* and Clark H Lewis†
ARO, Inc, Tullahoma, Tenn

Heat-transfer distribution data obtained on a 9° half-angle spherically blunted cone at Mach numbers near 20 and freestream Reynolds number between 8000 and 15,000/in in the hypervelocity (hotshot) tunnels are presented The test data are compared with Lees' laminar heat-transfer theory and available shock-tunnel data on similar cones Good agreement between Lees' theory and the experimental data is obtained Experimental pressure and heat-transfer distributions were correlated over a wide range of nose-bluntness ratios, cone half-angles, and Mach numbers by modifying the correlation parameters proposed by Cheng A simple formula is given which is adequate for engineering estimates of the heat-transfer rate to the conical afterbody of a spherically blunted cone at hypersonic conditions

Nomenclature

C = correlation constant [Eq (8)]
C_* = form of Chapman Rubesin viscosity coefficient, $\mu_*/\mu_\infty = C_*T_*/T_\infty$
C_H = heat-transfer coefficient, $\dot{q}_w/\rho_\infty U_\infty(h_0 - h_w)$
C_p = pressure coefficient, $(p - p_\infty)/q_\infty$
c_p = specific heat at constant pressure
D_B = base diameter, in
d = nose diameter, in
g = $C_p/2\theta_c^2$
h = enthalpy of gas, ft²/sec²
h_r = Wilson's reference enthalpy [Eq (5)]
K = constant in Fay-Riddell equation [Eq (2)]
k = nose-drag coefficient (0 964 for spherically blunted cone)
L = model length, in
M = Mach number
p = pressure
Pr = Prandtl number
q_∞ = dynamic pressure, $\rho_\infty U_\infty^2/2$
$\dot{q}$ = heat transfer rate, Btu/ft²-sec
$\dot{q}_0$ = stagnation heat-transfer rate behind a normal shock
$\dot{q}_0$ = computed stagnation heat transfer rate [Eq (2)]
$\dot{q}_{0w}$ = inferred stagnation heat rate, $\dot{q}_w/(\dot{q}/\dot{q}_0)_{\text{Lees}}$ $(\dot{q}/\dot{q}_0 =$ 0 0465 for a hemisphere-cylinder at $S/R_0 = 2\,32$, $M_\infty \sim 18)$
R = radius, in
R_B = base radius, in
R_0 = nose radius, in

Received July 29, 1963; revision received December 13, 1963 This work was sponsored by the Arnold Engineering Development Center, Air Force Systems Command, U S Air Force, under Contract AF 40(600)-1000 with ARO, Inc, Operating Contractor, AEDC

* Supervisor, Aerodynamics Section, Hypervelocity Branch, von Kármán Gas Dynamics Facility

† Engineer, Special Projects Section, Hypervelocity Branch, von Kármán Gas Dynamics Facility Member AIAA

Re = freestream Reynolds number
Re_∞/in = freestream Reynolds number per inch
$Re_{\infty\, d}$ = freestream Reynolds number based on nose diameter
S = entropy
s = surface distance from stagnation point of model, in
T = temperature, °K
T_* = reference temperature $(T_0/6)(1 + 3T_w/T_0)$, Ref 8
t = time
U = velocity, fps
W_1, W_2 = parameters defined in Eq (5)
X = Cheng s axial distance parameter, $(x/d)\theta^2/(\epsilon k)^{1/2}$
x = axial distance, in
Y = Cheng s modified heat transfer parameter [see Eq (3)]
Z = compressibility factor
γ = ratio of specific heats c_p/c
ϵ = $(\gamma - 1)/\gamma + 1$
θ_c = cone half-angle, radians unless otherwise noted
μ = gas viscosity
ξ = s/R_0
ρ = density, slugs/ft^3
ψ = nose bluntness, R_0/R_B

Subscripts

AC = based on computed average conditions in arc-chamber
a = conditions at 1 atm pressure and 273 16°K
adw = adiabatic wall conditions
BW = blast-wave velocity (measured)
e = local conditions at the edge of the boundary layer
i = initial conditions
0 = freestream stagnation conditions
0′ = stagnation conditions behind a normal shock
$\dot{q}_0$ = based on measured stagnation heat-transfer rate
$\dot{q}_{0w}$ = based on inferred stagnation heat-transfer rate
r = condition at reference enthalpy h
w = wall conditions
∞ = freestream conditions
$*$ = conditions at reference temperature T_*

Superscript

(m) = number of iterations

Introduction

IN general studies of practical hypersonic flow situations, it is desirable to choose a body geometry that clearly simulates the physical conditions of interest and also is amenable to theoretical investigation For high speed, high-altitude flight through the atmosphere, the body must be blunted to reduce the aerodynamic heating Moreover, to reduce the drag and thus increase the speed, the afterbody should also be rather slender One such body that has been studied, both experimentally and analytically, is a spherically blunted cone

Experimental studies have been conducted on 9° half angle spherically blunted and/or flat-nosed cones by Lewis,[1] Whitfield and Norfleet,[2] Whitfield and Wolny,[3] and Whitfield and Griffith[4] in the hypervelocity (hotshot-type) tunnels of the von Kármán Gas Dynamics Facility, Arnold Engineering Development Center These studies included pressure distribution, shock shape, static stability, and zero-lift drag experiments in the nominal Mach number range 17–20, and freestream Reynolds number per inch between 8000 and 65,000 These studies were conducted in nitrogen

The method of characteristics has been used extensively to solve the hyperbolic partial differential equations that describe the supersonic flow field The procedure, even for an equilibrium dissociating and ionizing gas, is relatively straightforward However, various methods have been devised to obtain the necessary starting data; those most commonly used are the integral method of Dorodnitsyn-Belotserkovskii,[5] the inverse method of van Dyke,[6] and the transonic flow-field method of Gravalos et al[7]

The analytical results of the General Electric Company using the method of Gravalos et al[7] for a 0 3 bluntness ratio (ψ) spherically blunted 9° half-angle cone have been used extensively It was, in fact, the availability of these data which prompted the selection of this specific shape It is worth noting here, however, that the numerical results of the General Electric Company were for equilibrium dissociating air properties, whereas the experiments were conducted in nitrogen at conditions such that the effects of dissociation are much less than those in the air calculations One should thus apply caution when comparing the inviscid analytical and experimental results

Cheng[8] theoretically investigated the effects of nose bluntness on shock shape, pressure distribution, and surface heat-transfer rate over blunted slender cones The flow model he considered consisted of three adjoining regions: 1) an inner laminar boundary layer; 2) an outer detached shock layer; and 3) between 1 and 2, a low-density entropy layer

The laminar heat-transfer theory of Lees[9] has been very successful in predicting the heat-transfer rate over blunt bodies at low Mach numbers as, e g , in shock-tube experiments Moreover, even when the pressure gradient, whose effect is neglected in the theory, is quite large, the theory will be shown to be satisfactory in predicting heat-transfer rates to slender, blunted cones

A brief description will be given of the wind tunnel, test conditions, and model instrumentation However, primary attention will be given to 1) the method used to determine the flow conditions in the hotshot wind tunnels, 2) the precision of the measured data, 3) theoretical considerations related to the correlation of the pressure and heat transfer distribution, and 4) a comparison of the theories and experiment

It will be shown that modifications of Cheng's pressure and heat-transfer correlation parameters will permit the experimental data to be correlated over a wide range of Mach numbers, cone half-angles, and nose-bluntness ratios

Test Apparatus and Models

The experimental data reported here were obtained in two of the hypervelocity (hotshot) tunnels of the Arnold Engineering Development Center-von Kármán Facility (AEDC-VKF), and typical test conditions are shown in Table 1 These tunnels, shown in Fig 1, are electric arc-heated hypersonic wind tunnels using nitrogen as a test gas and equipped with conical nozzles Stagnation temperatures were such that theoretical liquefaction of the gas in the test-section was avoided As shown in Table 1, the range of freestream Mach numbers M_∞ was small, and thus the principle quantity varied was freestream Reynolds number Re Detailed descriptions of these tunnels can be found elsewhere [10–14]

Experimental data[15, 16] are also shown from the Cornell Aeronautical Laboratory (CAL) 11 × 15 and 48-in shock tunnels using air as the test gas The test conditions relative to the CAL data will be given on the figures where the data are presented

Table 1 Typical test-section and stagnation conditions in the hypervelocity (hotshot) tunnels

Test section diam	M_∞	p_0, psia	T_0, °K	Re_∞/in × 10^{-3}
100-in (F)	20	7400–7700	3300–4000	8–11
50-in (H)	19	6000–7000	2800–3700	9–15

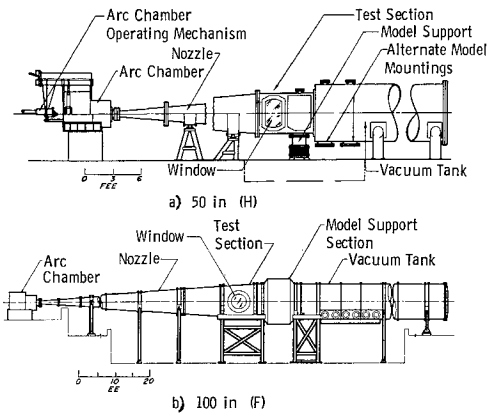

Fig 1 AEDC-VKF hypervelocity (hotshot) tunnels

The 9° half-angle cone (Fig 2) was fabricated of type 303 nonmagnetic stainless steel and was instrumented with VKF heat-transfer gages[17] and wafer-type pressure transducers [18] The heat-transfer gage consists of a copper disk held in place by a thermally insulating material with a thermocouple soldered to the back face to sense the disk temperature The gage thickness was tailored to the expected level of heat-transfer rate to be measured The stagnation-point gage was 0 020 in thick, whereas the other gages were 0 003 in thick Calibration of the thermocouple gages with a torch flame and standard calorimeter was within ±10% of the theoretical calibration factors based on disk mass, specific heat, and thermocouple output

Precision

Flow Conditions

Until recently, flow conditions were determined as described in Ref 19 This method is summarized as follows: 1) measure initial pressure and density in arc-chamber, p_{0i} and ρ_{0i}; 2) calculate initial enthalpy, entropy, and temperature, h_{0i}, S_{0i}, and T_{0i}; 3) measure timewise decay of pressure in arc-chamber, dp_0/dt; 4) calculate timewise decay of density in arc-chamber; 5) calculate timewise decay of enthalpy, entropy, and temperature; 6) measure instantaneous pitot pressure in test-section, p_0'; 7) calculate instantaneous values of flow conditions in test-section (M, Re, etc) based on instantaneous values of ρ_0, p_0, T_0, h_0, S_0, and p_0', assuming an equilibrium isentropic expansion from arc-chamber to test-section; and 8) complete space uniformity of gas properties in the arc-chamber (T_0, ρ_0, p_0) are necessarily assumed in this method

Experiments in which instantaneous flow velocity was measured from the translation of blast waves through the test-section showed that velocity calculated as just described frequently differed radically from the measured velocity These experiments also showed that the velocity calculated from measured heat transfer rates was in good agreement with the measured blast-wave velocity These experiments are described in Ref 12, and results are summarized in Fig 3 Referring to Fig 3, it is seen that the velocity determined from stagnation-point heat-transfer rates measured at the nose of a hemisphere-cylinder ($\dot{q}_0$) or inferred from heat-transfer rates measured beyond the shoulder of the hemisphere ($\dot{q}_{0w}$) agreed with the measured blast-wave velocity within ±5%

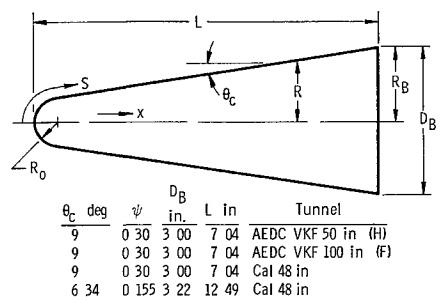

θc deg	ψ	DB in.	L in	Tunnel
9	0 30	3 00	7 04	AEDC VKF 50 in (H)
9	0 30	3 00	7 04	AEDC VKF 100 in (F)
9	0 30	3 00	7 04	Cal 48 in
6 34	0 155	3 22	12 49	Cal 48 in

Fig 2 Spherically blunted cone models

Figure 4 presents typical timewise velocity data Note that the agreement between the velocity measurements $U_{\dot{q}0}$ and U_{BW} is excellent even when the velocity U_{AC} is radically different Clearly, the earlier method frequently yielded erroneous flow conditions

The foregoing results show definitely the existance of significant enthalpy gradients in the arc-chamber caused by incomplete heating of the gas The results also show the advantage of experimental determination of freestream conditions from pitot pressure and stagnation heat transfer rate rather than the average computed arc-chamber enthalpy and pitot pressure

A revised method for determining flow conditions has been adopted and was used in this investigation Briefly, this method is summarized as follows:

1) Instantaneous values of p_0 and p_0' were measured

2) Instantaneous values of $\dot{q}_0$ were either measured directly or inferred from a measurement of $\dot{q}_w$ using Lees' distribution theory[9] with experimental pressure distribution

3) Enthalpy (h_0) was calculated from an approximate equation of the form $h_0^{(1)} = f(p_0', \dot{q}_0)$ With values of p_0, p_0', and h_0 known, the remaining flow conditions (M, Re, etc) were calculated as described in Ref 19 for an equilibrium isentropic expansion

4) Using the calculated flow conditions, $\dot{q}_0$ was calculated from Fay-Riddell theory[20] and compared to the measured $\dot{q}_0$, and the procedure was repeated with a corrected h_0 adjusted by the differences in computed and measured $\dot{q}_0$ ($h_0^{(m+1)} = h_0^{(m)} \dot{q}_0 / \dot{q}_{0c}$) The iteration was repeated until the measured $\dot{q}_0$ and the calculated $\dot{q}_0$ were in agreement within 1%

5) Newtonian pressure distribution near the stagnation point and unit Lewis number were assumed in the Fay-Riddell theory

Use of this revised method has greatly improved the consistency of results for the VKF hotshot tunnels and has simplified calculation of flow conditions in that the laborious calculation of timewise decay of density in the arc-chamber has been eliminated

The dual-gage heat-transfer probe used to measure $\dot{q}_0$ and $\dot{q}_w$ also serves as an excellent contamination monitor If solid particle contamination is present in the flowing gas, the measured value of $\dot{q}_0$ will be higher than the correct

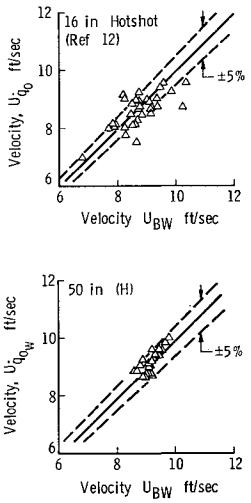

Fig 3 Comparison of measured and calculated flow velocity based on arc-chamber and blast-wave velocity measurements

Table 2 Precision of heat-transfer and pressure data

Hypervelocity tunnels	Probable error, %	
	Pressure	Heat transfer
50-in (H)	±5	±10
100-in (F)	±5	±10

value because of particle impingement at the nose of the probe, whereas the influence of solid particles on gages aligned with the flow (i e , aft of hemisphere-cylinder junction) must be of second-order as compared to the influences at the stagnation point Thus, a comparison of the measured $\dot{q}_0$ with a value of $\dot{q}_{0w}$ inferred from the measured value of $\dot{q}_w$ will indicate a presence of, or lack of, particles in the flow Typically these values agree within ±10%, indicating negligible solid particle contamination Occasionally these measurements indicate a "dirty" run The frequency of such occasions was small, and data from such runs were not used

Measured Data

The precision of the heat-transfer and pressure data ob tained in the present investigation was estimated, and the results are shown in Table 2 (for an approximate 90% confidence level) The ±5% spread of flow velocities inferred from stagnation heat rates as compared to measured flow velocities (see Fig 3) corresponds to the ±10% spread in the heat-rate data, whereas the variable-reluctance pressure transducers are linear within ±2% and have an over-all repeatability in p/p_0' of ±5%

All of the data presented herein were obtained in conical nozzles Whitfield and Norfleet[2] discussed the influence that source flow effects have on pressure measurements over slender sharp cones in conical hypervelocity nozzles No corrections for possible source flow effects were made to the results presented herein since they were considered to be negligible

Theoretical Considerations

Pressure Distributions

The correlation of pressure distributions in terms of parameters proposed by Cheng[8] was used to specify the pressure distributions for the blunted cones considered in this paper The data of Lewis[1] and CAL[16] were replotted along with other VKF data in terms of pressure coefficient as shown in Fig 5 Note that these data show no dependence of pressure coefficient on Mach number Cheng's parameter $p_w/M_\infty^2 p_\infty \theta^2 \gamma_\infty$ is, of course, equivalent to $C_p/2\theta^2$ when $p_w \gg p_\infty$ For slender cones at only moderate hypersonic Mach numbers (~10), this condition cannot be satisfied; thus the use of $C_p/2\theta^2$ is expected to be more general, and the correlation of the available experimental pressure data (Fig 5) bears out this expectation

As shown in Fig 5, the General Electric Company's real-gas (air) characteristics solution[1 6] and the sharp cone value of Whitfield and Norfleet[2] agree well with the experimental data All numerical calculations (except the conical shock values) were made using this characteristics solution and the experimental sharp cone value[2] together with an approximate interpolation curve Shown also in Fig 5 is the perfect-gas, theoretical sharp cone (with attached conical shock) value for $M_\infty = 15$ and $\theta_c = 9°$

Heat-Transfer Calculations

Blunted cones

The heat-transfer computations were made using Lees' theoretical distribution[9] over the cone surface The pressure distribution was obtained from Fig 5 and modified Newtonian over the spherically blunted nose Local conditions at the edge of the boundary layer (denoted by subscript e) were calculated for an isentropic expansion from the stagnation conditions behind a normal shock [denoted by $(\ )_0'$]

Lees' equation is

$$\frac{\dot{q}_w}{\dot{q}_0} = \frac{\frac{1}{2}\frac{p_w}{p_0'}\frac{U}{U_\infty}\frac{R}{R_0}}{\left\{\int_0^\xi \frac{p_w}{p_0'}\frac{U_e}{U_\infty}\left(\frac{R}{R_0}\right)^2 d\xi\right\}^{1/2}} \left\{\frac{U_\infty^2 \rho_0'}{2(p_0' - p_\infty)}\right\}^{1/4} \tag{1}$$

The stagnation-point heat-transfer rate was calculated based upon the Fay-Riddell[20] theory for a 300°K wall temperature The equation used was

$$\dot{q}(R_0)^{1/2} = K\left(\frac{\rho_w}{\rho_a}\right)^{0.1}\left(\frac{\rho_0}{\rho_a}\mu_0'\right)^{0.4}(h_0 - h_w)\left(\frac{p_0' - p_\infty}{\rho_0'/\rho_a}\right)^{0.25} \tag{2}$$

where $K = 1.7044 \times 10^{-3}$ for nitrogen, $K = 1.7247 \times 10^{-3}$

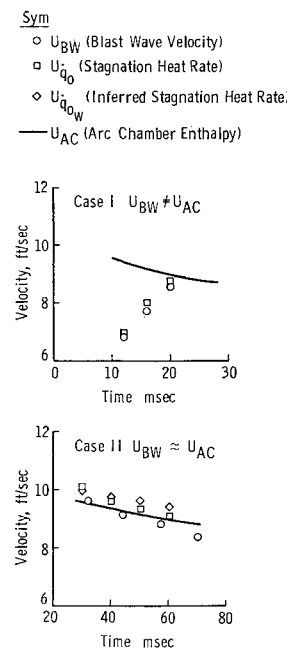

Fig 4 Typical timewise data comparison of measured and calculated flow velocity based on arc-chamber and blast-wave velocity measurements

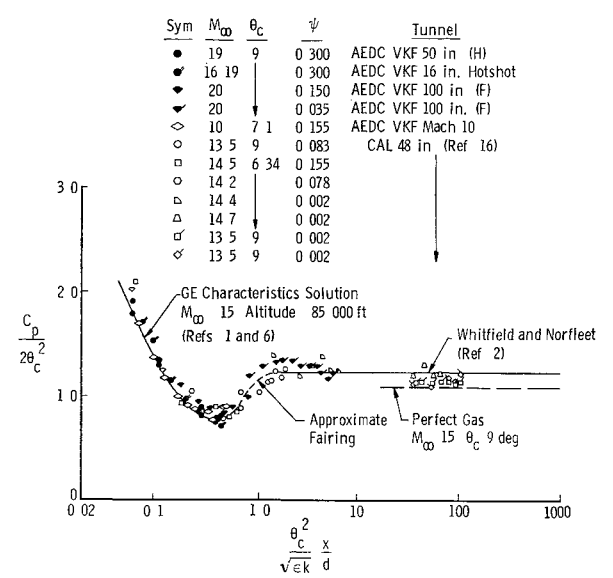

Fig 5 Correlation of zero-lift cone pressures, M_∞ = 10 to 20

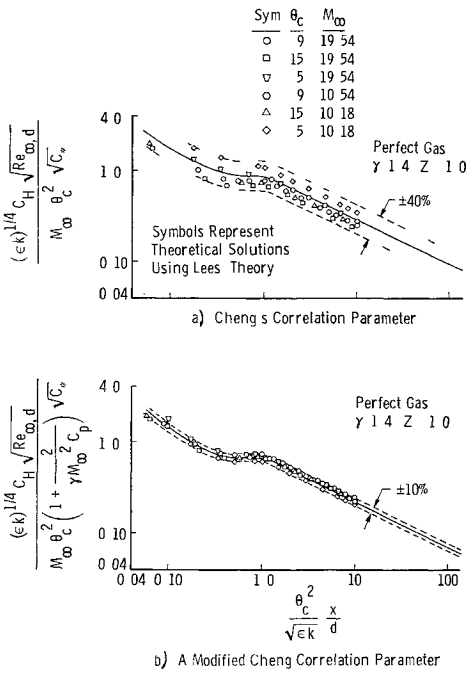

Fig 6 Theoretical heat-transfer rates to blunted cones based on Lees' heat-transfer distribution

for air, the dimensions of $\dot{q}_0(R_0)^{1/2}$ are Btu-(in)$^{1/2}$/ft^2-sec, and the pressure is in atmospheres

The heat-transfer calculations were made considering both perfect-gas and real-gas properties [21 22] All calculations were for stagnation temperatures of 4000°K or less As noted by Kemp, Rose, and Detra,[23] the effect of γ on heat-transfer distributions was negligible The ratio of specific heats (γ) affects the test-section parameters during isentropic nozzle flow expansions and thereby would have some influence upon Cheng's correlation parameter However, for the conditions covered in this paper these effects were only about 5%

Cheng,[8] in the development of his theory, assumed p_w/p_0' constant with Mach number and proportional to θ_c^2 for $M_\infty^2\theta_c^2 \gg 1$ Figure 5 indicates that $C_p/2\theta^2$ is independent of M_∞ at hypersonic conditions As noted previously, Cheng's parameter implies that $p_w \gg p_\infty$; thus, expressing

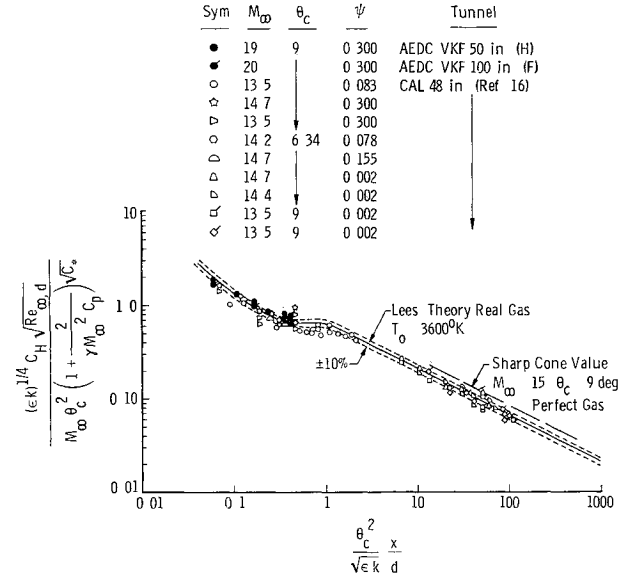

Fig 7 Comparison of theoretical and experimental heat-transfer rates to spherically blunted cones

the heat-transfer data in terms of Cheng's correlation parameter results in curves (see Fig 6a) with a Mach number and cone angle dependence and converging at high Mach numbers and larger cone angles This dependence is caused by the strong influence that p_∞/p_0' has at the lower hypersonic Mach numbers and on the more slender half angle cones A modification of Cheng's heat-transfer parameter can be accomplished to account for the fact that p_w is not always much larger than p_∞ Instead of assuming, as Cheng does, that $p/p_0' \propto \theta^2$, use the relation

$$2p_w/p_0' \simeq C_p + 2/\gamma M_\infty^2$$

or

$$p_w/p_0' \propto (\theta^2 + 1/\gamma g M_\infty^2)$$

where $g \equiv C_p/2\theta^2$, which is, as shown in Fig 5, a unique function of Cheng's distance parameter $(x/d)\theta^2/(\epsilon k)^{1/2}$ The modified version of Cheng's heat-transfer correlation then becomes

$$Y \equiv \frac{(\epsilon k)^{1/4} C_H (Re_{\infty,d}/C_*)^{1/2}}{M_\infty(\theta_c^2 + 1/\gamma g M_\infty^2)} \tag{3}$$

The numerical solutions in Fig 6a are presented in Fig 6b in terms of this modified correlation parameter where the improvement in using the modified correlation is apparent

Sharp cones

Soloman[24] gives the following formula for the heat transfer rate to a sharp cone (with attached conical shock) in an equilibrium real gas:

$$\dot{q}_w = 0\ 575\ Pr^{-2/3}(h_{dw} - h_w)(\rho\ \mu\ U/s)^{1/2} \tag{4}$$

where $\rho\ \mu$ is evaluated at the Wilson[25] reference enthalpy

$$h = 0\ 9W_1(h_w + h_e) + 1\ 08W_2(U^2/2) + h\ (1 - 1\ 8W_1) \tag{5}$$

where

$$W_1 \equiv 1 - \tfrac{1}{2}(Pr_r)^{1/4}$$
$$W_2 \equiv (Pr)^{1/2}[\tfrac{1}{2}(Pr_r)^{1/4} - \tfrac{1}{8}(Pr_r)^{1/3}]$$

Substitution of Eq (4) into the modified Cheng correlation parameter, Eq (3), yields

$$Y = 0\ 575\ Pr^{-2/3}\left(\frac{\rho_r\mu_r}{\rho_\infty\mu_\infty}\frac{U_e}{U_\infty}\frac{\cos\theta}{X}\right)^{1/2} \times \theta_c\{M_\infty C_*^{1/2}[\theta^2 + (\gamma M_\infty^2 g)^{-1}]\}^{-1} \tag{6}$$

where

$$X \equiv (x/d)\theta_c^2/(\epsilon k)^{1/2}$$

For the conditions considered here (perfect gas, $5° \leq \theta$

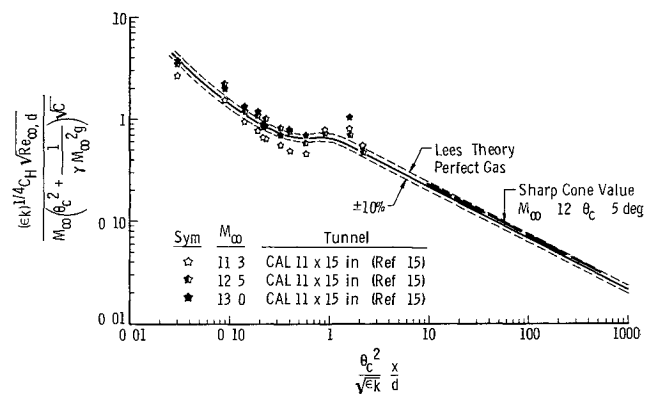

Fig 8 Comparison of theoretical and experimental heat-transfer rates to flat-nosed cones

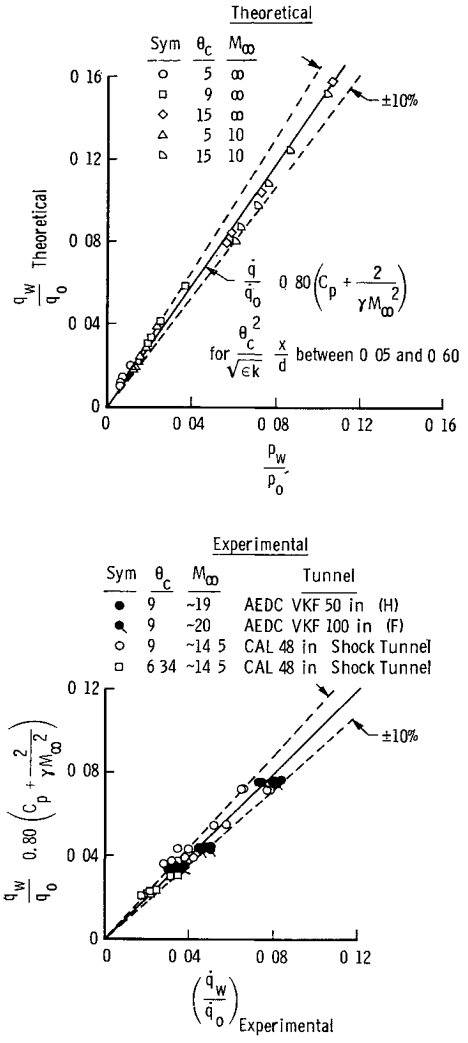

Fig 9 Correlation of blunt cone heat-transfer distribution data

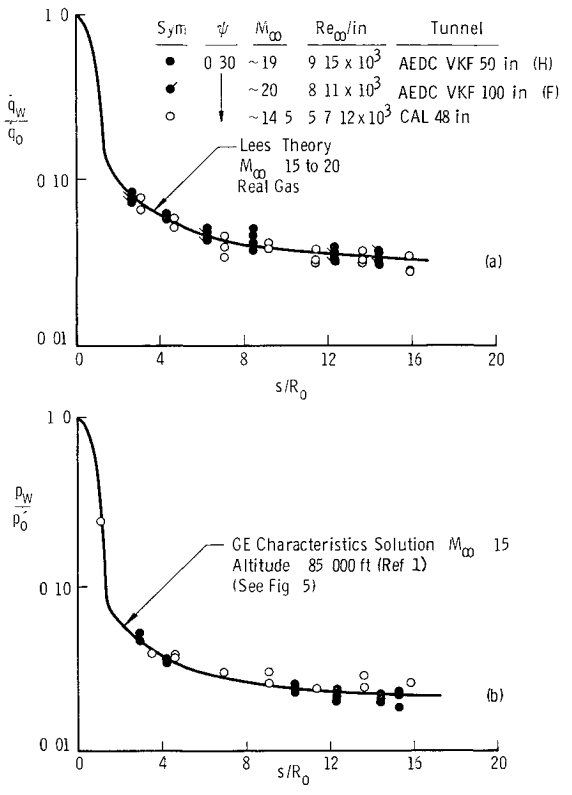

Fig 10 Heat-transfer and pressure distributions over a 9° half-angle spherically blunted cone

$\leq 15°$, $10 \leq M_\infty \leq 20$), it was found that $h = c_p T_*$ within a percent or so A comparison of the definition of Cheng's[8] T_* with Wilson's[25] T_r clearly indicates this Thus, for $Pr_r = 0\,71$ (const), Eq (6) becomes

$$Y(X)^{1/2} = \frac{0\,7224\{(U_e/U_\infty)[\cos\theta_c/(p_w/p_\infty)]\}^{1/2}[(p_w/p_\infty) - 1]}{M_\infty \theta_c} \quad (7)$$

One thus sees that $Y = Y(X^{-1/2};\ M_\infty, \theta)$ for a sharp cone and is, of course, now independent of the nose diameter

Results and Discussion

The experimental heat-transfer rates are shown in Figs 7 and 8 in terms of the modified Cheng correlation parameter Experimental points include data from the VKF tunnels, data of Wittliff and Wilson[15] for a 5° half-angle flat-nose cone, and CAL data[16] on spherically blunted cones

Figure 7 presents data for slender cones with spherically blunted noses in terms of the modified Cheng parameter Note the agreement between the experimental data and the theory for cones over a wide range of nose-bluntness ratios The numerical computation of Lees' theory in Fig 7 includes real-gas effects; however, as previously noted, within the flow region covered by this paper the real-gas effects change the theoretical calculations by only about 5%

The good agreement between Lees' theory and the sharper 6 34° and 9° cones must be considered, at present, fortuitous Certainly, the normal shock approximation used in calculating the local flow properties over the cone should be invalid for the sharper cones However, Whitfield and Griffith[4] reported similarly good agreement between theoretical estimates (normal shock theory) and experimental cold-wall zero-lift drag data from sharp cones Figure 7 also presents a theoretical solution for a conical shock case ($M_\infty = 15$, $\theta = 9°$) This case simply assumes that the cone surface pressure is constant at its inviscid value Solutions for other Mach numbers and cone half-angles were obtained (but not shown here), and they fell within ±10% of the theoretical sharp cone value shown

Comparison of the flat-nosed cone data of Wittliff and Wilson[15] with Lees' theory is shown in Fig 8 The data have been corrected to correspond to the definition of the reference temperature (T_*) used herein The constant 3 was inadvertently dropped in the original machine data reduction,[26] and this amounts to about a 4% correction In the calculation of the theory, a spherically blunted nose was assumed

The heat-transfer data were plotted as a function of the pressure ratio p_w/p_0', and these data are shown in Fig 9a From these data, the relation $\dot{q}_w/\dot{q}_0 \propto p_w/p_0'$ is clearly suggested Expressing p_w/p_0' in terms of C_p, one obtains

$$\dot{q}_w/\dot{q}_0 = C(q_\infty/p_0')[C_p + 2/\gamma M_\infty^2] \quad (8)$$

where C is a correlation constant to be determined From the perfect-gas ($\gamma = 1\,4$) solutions, $C = 1\,47$ and $q_\infty/p_0' = 0\,5436$ for $M_\infty \to \infty$ The final result is

$$\dot{q}_w/\dot{q}_0 = 0\,80(C_p + 2/\gamma M_\infty^2) \quad (9)$$

A comparison of the theoretical heat-transfer distribution with Eq (9) is shown on Fig 9a for $(x/d)\theta^2/(\epsilon k)^{1/2}$ between 0 05 and 0 60 ‡ From this comparison we see that Eq (9) is accurate within ±10% for $5 \leq \theta_c \leq 15°$, $M_\infty = 10$ and

‡ This corresponds approximately to the conical portion of the $\psi = 0\,3$ spherically blunted 9 half angle cone

∞ However, a more meaningful comparison is shown on Fig 9b where a comparison between Eq (9) and the experimentally measured heat transfer rate is shown All of the AEDC-VKF data are correlated by Eq (9) within $\pm 10\%$

The 50- and 100-in tunnel heat-transfer data are also presented in the form of ratios of measured surface-to-stagnation rate (Fig 10) This facilitates further use of the data and is also convenient for comparison directly with Lees' theory The measured heat-transfer rate distribution is compared to Lees' theory and data from CAL on a similar model Note the excellent agreement between Lees' theory and the VKF and CAL data

Conclusions

Based upon this investigation of heat-transfer to blunted slender cones at Mach numbers about 20 and Reynolds numbers per inch between 8000 and 15,000 in the AEDC-VKF hypervelocity (hotshot) tunnels, the following conclusions are made:

1) Good agreement between Lees' laminar heat-transfer theory and the experimental data for a 0 3 bluntness ratio spherically blunted 9° half-angle cone was obtained over the Reynolds number range investigated Good agreement was similarly obtained by comparison with the experimental data from AEDC-VKF and CAL shock tunnels The agreement between Lees' theory and the experimental data should, however, be considered somewhat fortuitous since the theory neglects the effects of pressure gradient

2) The pressure and heat-transfer distributions are independent of Mach number and cone angle when expressed in terms of a modification to the parameters proposed by Cheng [8]

3) A good engineering approximation for the heat-transfer distribution over slender blunted cones for $(x/d)\theta_c^2/(\epsilon k)^{1/2}$ between 0 05 and 0 60 is $\dot{q}_w/\dot{q}_0 = 0\,80\ (C_p + 2/\gamma M_\infty^2)$ This formula was derived in this investigation, and the result was tested for slender blunted cones at Mach numbers near 20 and found to be accurate within about $\pm 10\%$

References

[1] Lewis, C H, "Pressure distribution and shock shape over blunted slender cones at mach numbers from 16 to 19," Arnold Eng Dev Center TN-61-81 (1961)

[2] Whitfield, J D and Norfleet, G D, "Source flow effects in conical hypervelocity nozzles," Arnold Eng Dev Center TDR-62-116 (1962)

[3] Whitfield, J D and Wolny, W, "Hypersonic static stability of blunt slender cones, Arnold Eng Dev Center TDR 62-166 (1962)

[4] Whitfield, J D and Griffith, B J, "Viscous effects on zero-lift drag of slender blunt cones," Arnold Eng Dev Center TDR-63-35 (1963)

[5] Belotserkovskii, O M, "Flow with a detached shock wave about a symmetrical profile," PMM: J Appl Math Mech **22**, 279–296 (1958)

[6] van Dyke, M, "The supersonic blunt-body problem-review and extension," J Aerospace Sci **25**, 485–496 (1958)

[7] Gravalos, F G, Edelfelt, I H, and Emmons, H W, "The supersonic flow about a blunt body of revolution for gases at chemical equilibrium," General Electric Co R58SD245 (1958)

[8] Cheng, H K, "Hypersonic flow with combined leading-edge bluntness and boundary-layer displacement effect," Cornell Aeronaut Lab Rept AF-1285-A-4 (1960)

[9] Lees, L, "Laminar heat transfer over blunt-nosed bodies at hypersonic flight speeds," Jet Propulsion **26**, 259–268, 274 (1956)

[10] Lukasiewicz, J, Harris, W G, Jackson, R, van der Bliek, J A, and Miller, R M, "Development of capacitance and inductance driven hotshot tunnels," Arnold Eng Dev Center TN-60-222 (1961)

[11] Lukasiewicz, J, Whitfield, J D, and Jackson, R, "Aerodynamic testing at Mach numbers from 15 to 20," *ARS Progress in Astronautics and Rocketry: Hypersonic Flow Research*, edited by F R Riddell (Academic Press Inc, New York, 1962), Vol 7, pp 473–511

[12] Lukasiewicz, J, Jackson, R, and Whitfield, J D, "Status of development of hotshot tunnels at the AEDC," AGARD Meeting, Rhode-Saint Genese, Belgium, available from Arnold Eng Dev Center (April 1962)

[13] van der Bliek, J A, Deskins, H E, and Walker, R R, III, "Further development of an inductance-driven hotshot tunnel," Arnold Eng Dev Center TN-61-80 (1961)

[14] *Test Facilities Handbook*, von Kármán Gas Dynamics Facility, Arnold Eng Dev Center (July 1963), 5th ed, Vol 4

[15] Wittliff, C E and Wilson, M R, "An investigation of laminar heat transfer to slender cones in the hypersonic shock tunnel," Cornell Aeronaut Lab Rept AF-1270-A-2, Wright Air Dev Div TN-59-6 (1961); also "Heat transfer to slender cones in hypersonic air flow including yaw and nose-bluntness effects," IAS/ARS Preprint 61-213-1907 (1961); also "Heat transfer to slender cones in air flow including yaw and nose-bluntness effects," J Aerospace Sci **29**, 761–774 (1962)

[16] Wilkinson, D B and Harrington, S A, "Hypersonic force, pressure and heat transfer investigations of sharp and blunt slender cones," Cornell Aeronaut Lab Rept AF-1560-A-5 (1962)

[17] Ledford, R L, "A device for measuring heat-transfer rates in arc discharge hypervelocity wind tunnels," Arnold Eng Dev Center TDR-62-64 (1962)

[18] Smotherman, W E, "A miniature wafer-style pressure transducer," Arnold Eng Dev Center TR-60-11 (1960)

[19] Grabau, M, Humphrey, R L, and Little, W J, "Determination of test-section, after-shock, and stagnation conditions in hotshot tunnels using real nitrogen at temperatures from 3000 to 4000°K," Arnold Eng Dev Center TN-61-82 (1961)

[20] Fay, J A and Riddell, F R, "Theory of stagnation point heat transfer in dissociated air," J Aerospace Sci **25**, 73–85, 121 (1958)

[21] Hilsenrath, J, "A first approximation to the thermodynamic properties of nitrogen, Natl Bur Std, unpublished preliminary draft (1959)

[22] Landis, F and Nilson, E N, "Thermodynamic properties of ionized and dissociated air from 1500°K to 15,000°K, ' Pratt and Whitney Aircraft Rept 1921 (1961)

[23] Kemp, N N, Rose, P H, and Detra, R W, ' Laminar heat transfer around blunt bodies in dissociated air," J Aerospace Sci **26**, 421–430 (1959)

[24] Soloman, J M, "The calculation of laminar boundary layers in equilibrium dissociated air by an extension of the Cohen and Reshotko method," U S Naval Ordnance Lab TR-61-143 (1962)

[25] Wilson, R E, "Real-gas laminar-boundary-layer skin friction and heat transfer," J Aerospace Sci **29**, 640–647 (1962)

[26] Wittliff, C E, Cornell Aeronaut Lab, private communication (September 14 1962)